Simulation of Oil Separating Behavior for Engine Breather System

Makoto HAGA* Takumi KASAHARA**

ABSTRACT

The breather system of a reciprocating engine requires a function for separating the oil mist from the blow-by gas when ventilating the inside of the crankcase. Gas-liquid separation behavior inside the breather chamber is a complex phenomenon that involves liquid breakup and coalescence. Directly predicting this behavior by grid method, which is a typical numerical calculation method, is challenging, because the calculation grid deforms and moves excessively.

This study focused on a particle method suited to the analysis of complex fluid phenomena such as free surfaces and liquid breakup and coalescence, and attempted to predict the oil separating behavior of the breather chamber with the Moving Particle Semi-implicit method. An air resistance model was applied to accurately simulate particle motion based on the gas velocity field history that was calculated in advance by the grid method. In addition, a particle coarse-graining model was newly proposed to take into account the effect of air resistance on oil mist.

It was confirmed that the simulated oil scattering and separating behavior qualitatively agreed with the experimental results by high-speed camera, and that the oil separating behavior can be predicted by particle method.

1. Introduction

The inside of the crankcase of a reciprocating engine is filled with unburned gas and combustion gas (generally called “blow-by gas”) blown through from the combustion chamber. This produces issues such as increased pressure inside the crankcase that leads to oil leaks and the emission of atmospheric pollutants, dilution of the engine oil by the fuel and water vapor contained in the blow-by gas, and oil degradation by the NOx component in the gas. To address these issues, typical reciprocating engines are equipped with a breather system that ventilates the inside of the crankcase by discharging the blow-by gas to the intake manifold and taking fresh air into the crankcase. The blow-by gas contains large amounts of oil mist, and this mixing of oil to the intake manifold increases oil consumption, fouls the throttle valve and intake valve, and leads to a drop in emissions performance due to oil combustion. For these reasons, the breather chamber requires a function for separating the oil from the multiphase flow consisting of blow-by gas and oil mist.

Attempts have been made to predict and evaluate this oil separating function by the grid method, which is a typical numerical calculation method[(1), (2)]. However, dynamic behavior such as oil breakup and coalescence or oil adhered to the wall surfaces being carried away again by the gas flow is challenging to predict by calculation, because the calculation grid deforms and moves excessively. This means that there are still many unclear points regarding the oil separation behavior, and that all breather chamber specifications have not yet been determined by CFD.

This study focused on a particle method that calculates fluid motion using a Lagrangian approach by using particles to discretize the fluid without using a grid (Fig. 1). The

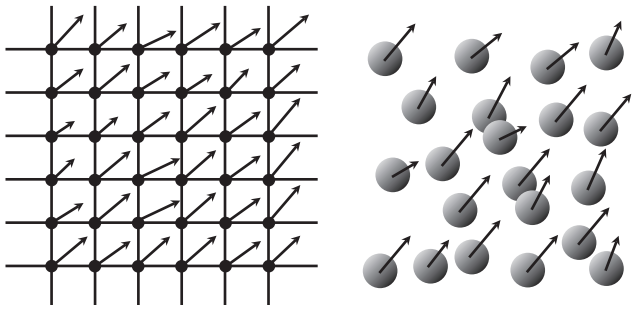

(a) Grid method (b) Particle method

Fig. 1 Concepts for grid and particle methods

* Automobile R&D Center

** Prometech Software, Inc.

particle method can directly extract the position of fluid using particles, so it is suited to analysis of complex fluids involving free surfaces, breakup and coalescence. This study used the fluid analysis software Particleworks[3] made by Prometech Software, Inc., which uses the Moving Particle Semi-implicit (MPS) method. In addition, an air resistance model, particle coarse graining model and surface tension model were introduced to create a method for analyzing the oil separating behavior inside the breather chamber.

2. Breather System

2.1. Overview of Breather System

Figure 2 shows an example of a breather system. Breather systems are also called Positive Crankcase Ventilation (PCV) systems, and ventilate the inside of the crankcase by using the negative pressure downstream from the throttle valve during partial load operation to discharge the blow-by gas to the intake manifold, and taking in fresh air from another passage upstream from the throttle. The blow-by gas flow rate is controlled by the PCV valve opening in accordance with the intake pressure. However, during idling or full-load operation the PCV valve is fully open, so the blow-by gas flows backward along the fresh air intake passage and is discharged to the intake manifold. In this case, the breather system has two blow-by gas discharge channels, and two breather chambers with oil separating functions are required.

2.2. Blow-by Gas and Oil Mist

The blow-by gas flow rate differs according to the engine displacement and the degree of piston ring and cylinder wear, and this flow rate can exceed 30 L/min for a 2 L inline 4-cylinder engine. The amount of oil mist contained in the blow-by gas differs greatly according to where the gas is taken from the engine, so the outlet port selection determines the amount of oil inflow to the chamber. The particle size of the oil mist in a gasoline engine has a distribution of approximately 1 μm to 10 μm.

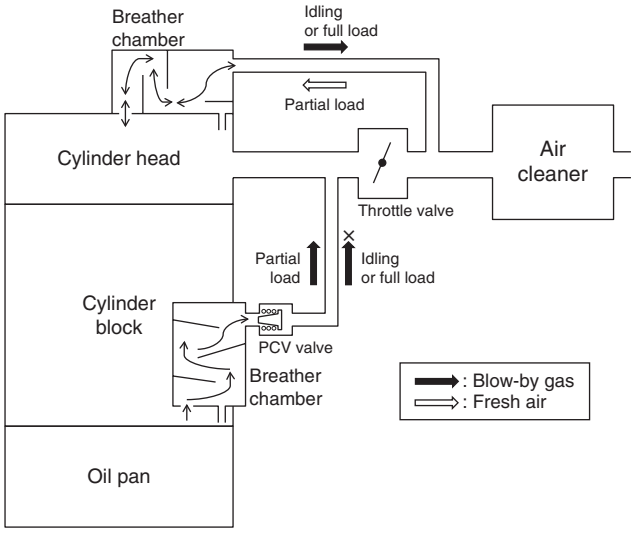

Fig. 2 Breather system

2.3. Oil Separation Methods

Oil separation methods are broadly divided into the labyrinth, impactor and cyclone types. Figure 3 shows examples of the labyrinth and impactor types. The labyrinth type has a long channel inside the chamber using partition plates and separates the oil mist by gravity as the gas flows along the channel. In contrast, the impactor type collides the gas with a collision plate and separates the oil mist using inertia. The cyclone type forms a swirling flow and separates the oil mist using centrifugal force.

3. Simulation Method

3.1. Overview of the MPS Method

The MPS method introduces semi-implicit algorithms for incompressible flows, and discretizes the governing equations by weighting the interactions between particles due to pressure and viscosity in accordance with the distance from particles existing within the effective radius r_e of the particle i shown in Fig. 4[4, 5]. The governing

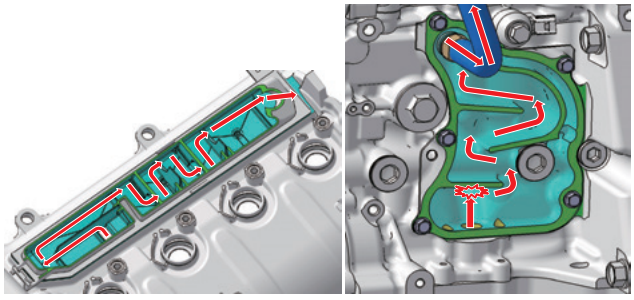

(a) Labyrinth type (b) Impactor type

Fig. 3 Breather chambers

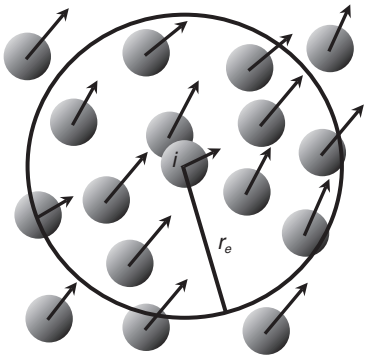

Fig. 4 Effective radius for MPS method

equations use the following equations described by the Lagrangian method. Equation (1) is an equation of continuity (Law of Conservation of Mass) and Eq. (2) is a Navier-Stokes equation (Law of Conservation of Motion).

$$\frac{D\rho}{Dt} = 0 \tag{1}$$

$$\frac{D\vec{u}}{Dt} = -\frac{\nabla P}{\rho} + \nu\nabla^2\vec{u} + \vec{g} \tag{2}$$

ρ: density, $\vec{u}$: velocity, P: pressure, ν: coefficient of kinematic viscosity
$\vec{g}$: gravitational acceleration, $\frac{D}{Dt}$: Lagrangian derivative

3.2. Application to Simulation of Oil Separating Behavior

The fluid inside the breather chamber is a gas-liquid multiphase flow consisting of blow-by gas and oil. In the particle method, when the behavior of fluids with greatly differing densities such as gas and liquid is calculated with particles, the pressure calculation becomes unstable[5]. Therefore, this study applied an air-resistance model to accurately simulate particle motion based on the gas velocity field history that was calculated in advance by the grid method. Figure 5 shows the simulation procedure. In addition, a particle coarse graining model and surface tension model were also introduced to enhance the particle behavior calculation accuracy. The contents of each model are described below.

3.2.1. Air-resistance model

In the air-resistance model, the particles move while satisfying the following Navier-Stokes equation Eq. (3), which adds a drag term to Eq. (2).

$$\frac{D\vec{u}}{Dt} = -\frac{\nabla P}{\rho} + \nu\nabla^2\vec{u} + \vec{g} - \frac{1}{m}\vec{D} \tag{3}$$

m: liquid mass, $\vec{D}$: drag

$\vec{D}$ is defined as shown by Eq. (4) below.

$$\vec{D} = \frac{C_D}{2}\rho_{air}\left|\vec{u}_l - \vec{u}_g\right|(\vec{u}_l - \vec{u}_g)\,S \tag{4}$$

C_D: coefficient of drag, ρ_{air}: mass density of air, $\vec{u}_l$: liquid velocity
$\vec{u}_g$: gas velocity, S: Liquid body surface area

3.2.2. Particle coarse graining model

In order to accurately calculate the motion of the oil mist, the size of the calculation particles (hereafter, "MPS particles") used by the MPS method should be the same as the particle size of the oil mist (1 μm to 10 μm). However, this would require a vast number of particles relative to the inflow oil volume, making it unlikely that results could be obtained within a practical period of time. In consideration of practicality, the particle size of MPS should be set to approximately 250 μm to 500 μm. Therefore, this study coarse grained the MPS particles as grouped droplets so that the effect of air resistance on the MPS particles is the same as that on the oil mist. Figure 6 shows a concept drawing of coarse graining. The relationship between the sizes of the coarse-grained MPS particles and the oil mist particles is as follows.

$$R_{cg} = \frac{D_l}{d_l} \tag{5}$$

$$N = R_{cg}{}^3 \tag{6}$$

R_{cg}: coarse graining ratio, D_l: particle size of MPS, d_l: particle size of oil mist
N: number of grouped droplets

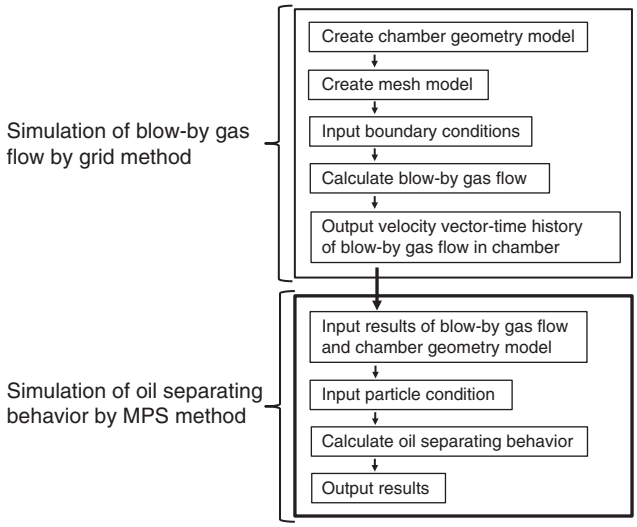

Fig. 5 Flowchart of simulation

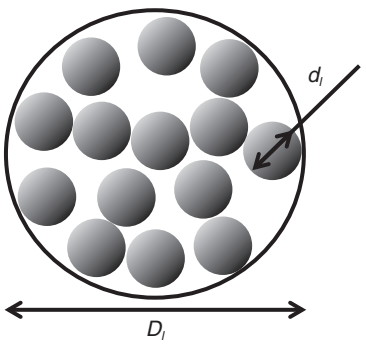

Fig. 6 Coarse graining model

In addition, the coefficient of drag C_D in Eq. (4) is given by Eq. (7) and Eq. (8) below[6].

$$Re = \frac{d_l \left| \vec{u}_l - \vec{u}_g \right|}{\nu_g} \tag{7}$$

$$C_D = \begin{cases} \dfrac{24}{Re}\left(1 + \dfrac{Re^{2/3}}{6}\right) & Re \le 1000 \\ 0.424 & Re > 1000 \end{cases} \tag{8}$$

Re: Reynolds number, ν_g: coefficient of kinematic viscosity of the gas

The air-resistance force applied to the coarse-grained MPS particles is the resultant force of the forces applied to N number of grouped oil mist particles, and the MPS particles move while satisfying Eq. (9) below.

$$\frac{D\vec{u}}{Dt} = -\frac{\nabla P}{\rho} + \nu \nabla^2 \vec{u} + \vec{g} - \frac{R_{cg}{}^3}{m_l} \vec{D} \tag{9}$$

m_l: oil mist mass

3.2.3. Surface tension model

A surface tension potential model was introduced to take into account the influence of the surface tension of the liquid in the gas-liquid separation process. Particles influenced by surface tension move while satisfying the following Navier-Stokes equation Eq. (10).

$$\frac{D\vec{u}}{Dt} = -\frac{1}{\rho} \nabla P + \nu \nabla^2 \vec{u} + \vec{g} + \nabla \Phi \tag{10}$$

The fourth term in Eq. (10) is the surface tension term of the potential model, and is calculated as shown by Eq. (11) and Eq. (12) below.

$$\nabla \Phi = \sum_{j \neq i} \frac{d\varphi}{dr_{ij}} \cdot \frac{\vec{r}_{ij}}{\left| \vec{r}_{ij} \right|} \tag{11}$$

$$\Phi = C\varphi \tag{12}$$

i, j: particle numbers, $\vec{r}_{ij}$: position vector from particle i to particle j

φ expresses the potential energy, and uses an original Prometech Software equation.

C is the potential coefficient that determines the size of the potential force, and the value is proportional to the coefficient of surface tension of the liquid.

In addition, the wettability between the particles and the wall surfaces was taken into account by using the potential coefficient C_{fs} in Eq. (13) below.

$$C_{fs} = \frac{1}{2}(1 + \cos\theta)\, C \tag{13}$$

θ: contact angle

3.3. Necessity of the Coarse-Graining Model

In order to verify the coarse-graining model, MPS particles with coarse graining not performed ($R_{cg} = 1$) and with the coarse graining ratio R_{cg} set to 100 were flowed into a simple shape chamber for which the gas flow was calculated in advance, and the particle behavior was compared. The initial interparticle distance (particle size of MPS) was 500 μm. Figure 7 shows the simulation results. When coarse graining is not performed ($R_{cg} = 1$), the MPS particles are equivalent to a 500 μm oil mist, which is larger than the particle size of the actual oil mist (1 μm to 10 μm). As a result, changes of the particle velocity due to air resistance were small, and the particles gradually cohered due to the surface tension and completely obstructed the inlet hole at the 0.5 s mark. In contrast, when the coarse graining ratio R_{cg} is 100, the effect of air resistance on the MPS particles is the same as that for a 5-μm equivalent oil mist, so the particles scattered inside the chamber without obstructing the inlet hole.

Based on the above results, the coarse-graining model was determined to be necessary in order to calculate the behavior of the oil mist in the blow-by gas. Therefore, subsequent calculations presuming a breather chamber were performed with the coarse-graining ratio set to $R_{cg} = 50$ and $R_{cg} = 100$, which are equivalent to oil mist particle sizes of 10 μm and 5 μm, respectively.

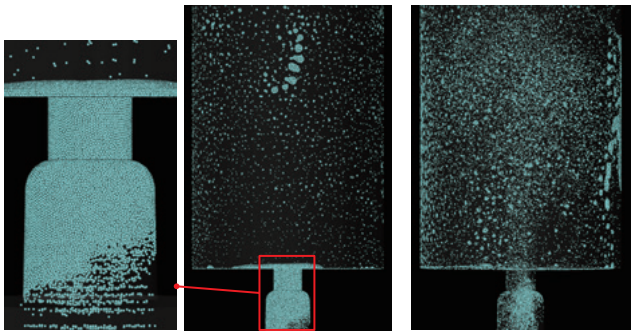

(a) $R_{cg} = 1$ [at 0.5 s] (b) $R_{cg} = 100$ [at 0.5 s]

Fig. 7 Comparison of particle movement between $R_{cg} = 1$ and $R_{cg} = 100$

4. Simulation of Oil Separating Behavior

4.1. Simulation Conditions

4.1.1. Simulation subject

In this study, the impactor-type separator of the breather chamber built into the cylinder block was selected as the simulation subject. Evaluation testing of the oil separation performance of the breather chamber was performed using the size of the blow-by gas inlet hole and distance to the first collision plate of an actual chamber as parameters,

Table 1 Specifications of breather chambers

Breather chamber	TYPE 1	TYPE2
Oil separation performance	Good	Poor
Volume [cm^3]	215	
Distance to first collision plate from inlet hole [mm]	30	15
(1) Blow-by gas inlet hole		
Diameter [mm]	15	6
(2) Blow-by gas outlet hole		
Diameter [mm]	7	
(3) Connecting channel to cylinder head		
Diameter [mm]	7	
(4) Oil drainage holes		
Diameter [mm]	8	

and two specifications with markedly different separation performance were compared. Figure 8 and Table 1 show the appearance and specifications of the compared chambers. TYPE1 has an inlet hole size of ϕ15 mm and a distance of 30 mm from the inlet hole to the first collision plate. TYPE2 has an inlet hole size of ϕ6 mm and a distance of 15 mm from the inlet hole to the first collision plate.

4.1.2. Calculation of the blow-by gas flow by the grid method

The gas flow inside the chamber was calculated by the grid method in order to calculate particle motion based on the gas velocity field history in the air-resistance model. The calculations applied the same conditions as the operating condition of an engine speed of 6000 rpm at which the maximum blow-by gas flow rate of 40 L/min was measured in the oil separation performance verification tests. The pressure pulsation inside the crankcase was set as the boundary condition for the gas inlet hole (1), atmospheric pressure was set as the boundary condition for the gas outlet hole (2) that was left open to the atmosphere during the tests, and the pressure pulsation inside the cylinder head was set as the boundary condition for the connecting channel (3). The oil drainage holes (4) connect into the oil in the oil pan, so a boundary condition was not set. Figure 9 shows the simulation results by the grid method. The gas periodically flowed into the chamber due to pressure pulsation, and the maximum collision velocity to the collision plate was 30 m/s for TYPE1 and 40 m/s for TYPE2. These results were input to Particleworks as the boundary conditions for the air-resistance model.

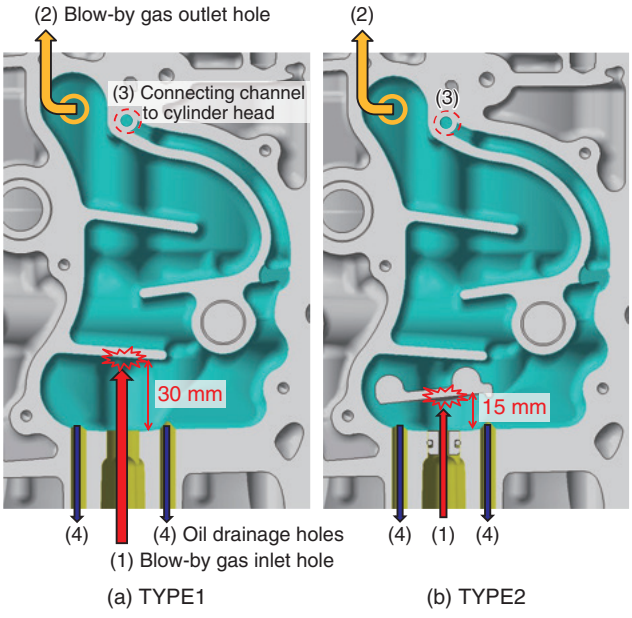

Fig. 8 Schematic of measured breather types

4.1.3. Simulation conditions for the particle method

The oil mist flow rate was assumed to be 1% of the volumetric flow rate of the blow-by gas, and the conditions were set so that MPS particles equivalent to that flow rate flowed into the chamber from the inlet hole (1) synchronized with the gas inflow speed. In addition, the coefficient of kinematic viscosity, coefficient of surface tension and contact angle of the oil at 80°C were input as the physical property values of the MPS particles. The particle size of MPS was 500 μm, and calculations were performed using the two conditions of a coarse graining ratio R_{cg} of 50 (equivalent to an oil mist particle size of 10 μm) and 100 (equivalent to 5 μm).

4.2. Simulation Results

4.2.1. Particle behavior

Figure 10 shows the behavior of the MPS particles in TYPE1 with a coarse graining ratio R_{cg} of 100. The MPS particles are indicated by velocity vectors, and the numbers in the figures correspond to the pressure pulsation phases in the graph above. The particles periodically flowed into the chamber and collided with the collision plate due to the effects of the gas flow that fluctuates in accordance with the pressure pulsation inside the crankcase.

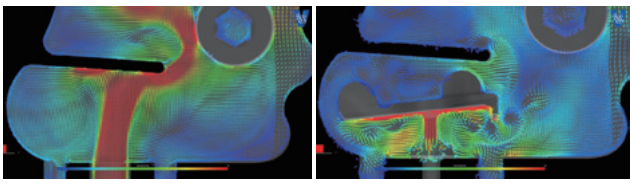

Fig. 9 Simulation results of flow in breather chamber by grid method

Figure 11 shows the behavior of the particles near the collision plate in TYPE1 and TYPE2. The arrows in the figures show the flow of the particles adhered to the wall surfaces. In TYPE1, the particles that collided with the collision plate were separated from the main gas flow and adhered to the right and left wall surfaces of the chamber. In particular, direction of movement of the particles from the right end of the collision plate was periodically changed by the influence of the pressure pulsation. In addition, the particles adhered to the right and left wall surfaces flowed along the wall surfaces toward the bottom of the chamber, forming a flow toward the oil drainage holes. In contrast, in TYPE2 it was confirmed that particles near the oil drainage holes were blown about by the gas flow, and in particular the particles adhered on the right wall surface did not flow toward the bottom of the chamber due to the effect of the gas flow deflected by the collision plate. Instead, the particles were blown upward again by the gas flow and flowed toward the downstream of the chamber. That is to say, TYPE2 can be judged to have a structure that makes it easy for separated oil to again become caught up in the airflow.

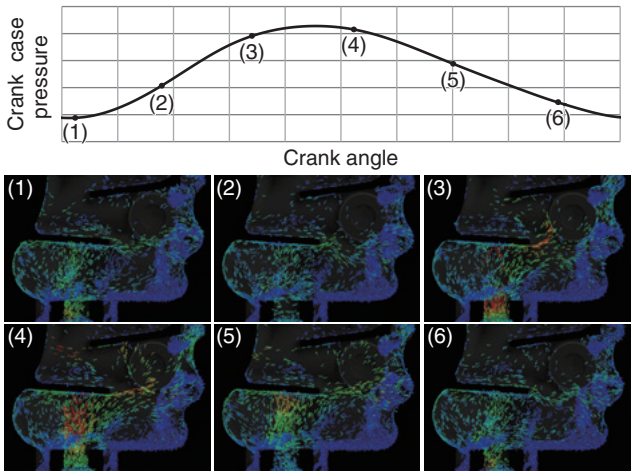

Fig. 10 Simulation results by MPS method [TYPE1, $R_{cg} = 100$]

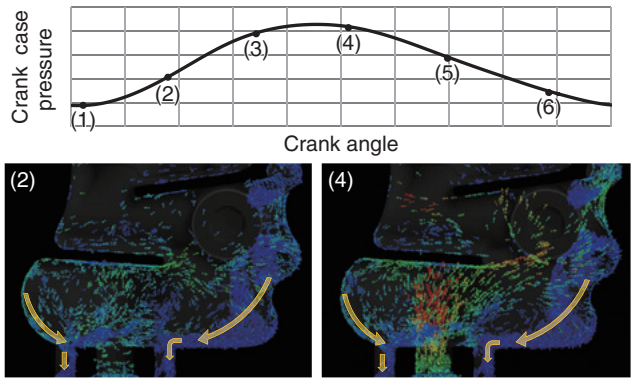

(a) TYPE1

(b) TYPE2

Fig. 11 Velocity vectors of MPS particles [$R_{cg} = 100$]

4.2.2. Differences in particle behavior by coarse graining ratio

Figure 12 shows the simulation results for a coarse graining ratio R_{cg} of 50 and 100 in TYPE1. Comparison of the particle behavior due to the difference in the coarse graining ratio showed that the particles scattered farther downstream when $R_{cg} = 100$, which corresponds to a 5-μm oil mist, and differing tendencies were also seen in the proportion of particles flowing to the right and left oil drainage holes.

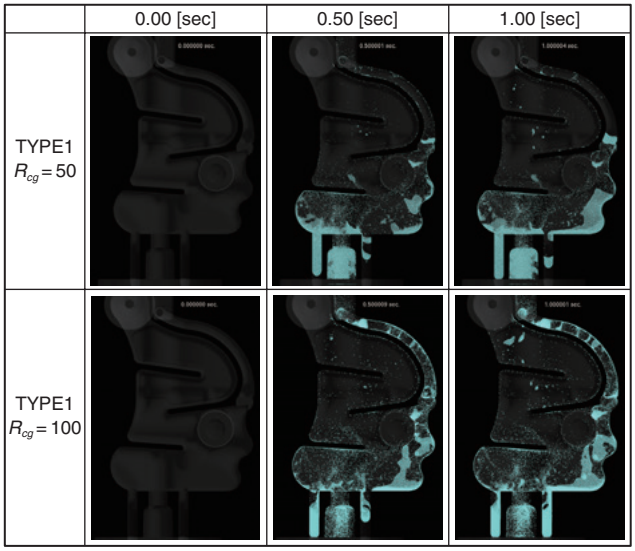

Fig. 12 Comparison of particle movement between $R_{cg} = 50$ and $R_{cg} = 100$

5. Verification and Examination of Simulation Results

5.1. Verification of Simulation Results by Actual Breather Chamber Visualization Tests

Actual breather chamber visualization tests were performed to verify the simulation results. The insides of the chambers were imaged for visualization by a high-speed camera while operating at an engine speed of 6000 rpm,

which is the same as the analysis condition at which a blow-by gas flow rate of 40 L/min was measured. The frame rate was 15000 fps and the shutter speed was 1/30000 s.

Figure 13 shows images of the visualization results with schematics representing the characteristic oil behavior. The numbers in the figures correspond to the pressure pulsation phases in the graph above. The oil mist was observed to periodically flow into the TYPE1 chamber, collide with the collision plate and scatter due to the pressure pulsation produced by volumetric changes inside the crankcase. In particular, due to the influence of changing direction of the gas flow by pressure pulsation, oil scattering direction at the right end of the collision plate was observed to change periodically. In addition, the oil adhered to the right and left wall surfaces of the chamber was observed to gradually fall toward the bottom of the chamber due to gravity. These tendencies agreed with the simulation results for both coarse graining ratios of 50 and 100.

On the other hand, although the oil mist was also observed to periodically flow into the TYPE2 chamber in the same manner as TYPE1, the oil was confirmed to accumulate and form a liquid lump at the bottom right of the chamber. This liquid lump did not flow toward the oil drainage holes due to the gas flow deflected by the collision plate, and was instead observed to be blown upward by the airflow, with part flowing toward the downstream of the chamber. Liquid lump formation was not observed in the simulation results for TYPE2, but a similar tendency was confirmed where the particles adhering to the right wall surface of the chamber accumulated without flowing toward the oil drainage holes, and the accumulated particles were blown upward again by the airflow and flowed to the downstream of the chamber. Therefore, the simulation results are thought to simulate the initial stage of liquid lump formation.

The above results showed that the simulated macroscopic oil behavior inside the breather chamber qualitatively agrees with experimental results. This confirmed that the macroscopic oil separating behavior inside a breather chamber can be predicted by introducing an air-resistance model, coarse-graining model and surface tension model to the MPS method.

5.2. Prediction of Oil Mist Behavior for Different Particle Sizes

The oil separation performance is thought to be affected by the particle size of the oil mist. Therefore, the total number of inflow particles and separated particles were

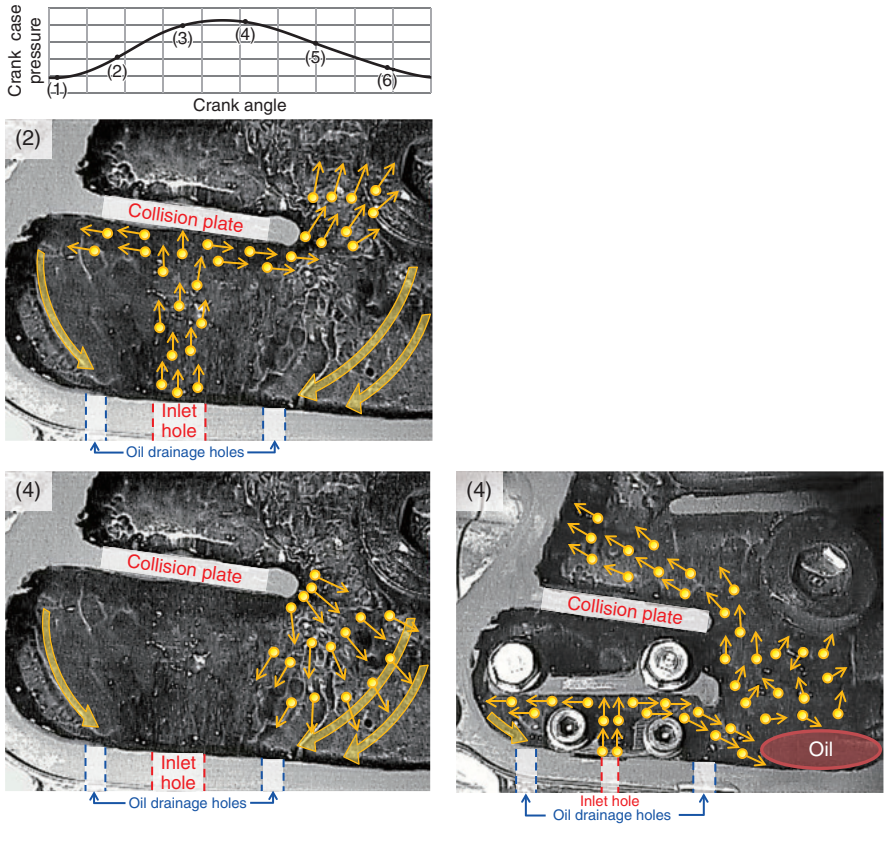

(a) TYPE1 (b) TYPE2

Fig. 13 Results of visualized measurement

counted for a coarse graining ratio R_{cg} of 50 (equivalent to an oil mist particle size of 10 μm) and 100 (equivalent to 5 μm), and the behavior of oil mists with different particle sizes was analyzed based on the results of calculations up to 1.0 s performed in this simulation. Figure 14 shows the inlet flow rate and separation flow rate time histories calculated from the number of inflow particles and the number of particles falling toward the right and left oil drainage holes for a coarse graining ratio R_{cg} of 50 and 100. Comparison of the inlet flow rate histories shows that a greater number of particles flow into the chamber when R_{cg} = 100, which corresponds to a 5-μm oil mist. This indicates that oil mist with a small particle size tends to easily flow into the chamber, and oil mist with a large particle size tends to be easily separated in the upstream region of the chamber (red frames in the figures). In addition, comparison of the flow-rate histories of the right and left oil drainage holes shows that more particles are separated from the left oil drainage hole when R_{cg} = 50, which corresponds to a 10-μm oil mist. This indicates that oil mist with a large particle size tends to collide with the collision plate, scatter toward the left side of the chamber and become separated from the main gas flow.

It is thought that the behavior of oil mists with different particle sizes can be analyzed by using the coarse graining ratio as a parameter as shown above. Thus, use of the developed method enables investigation of chamber structures in accordance with the particle size of the target oil mist.

6. Conclusion

A method based on the particle method was created for predicting the oil separating behavior of a breather system that was a challenge to analyze using the grid method, which is a typical numerical calculation method. The following results were obtained.

(1) A calculation method was created by introducing an air-resistance model, particle coarse-graining model and surface tension model to the MPS method as a means for predicting the oil separating behavior of a breather system.

(2) The simulated oil scattering and separating behavior inside the breather chamber qualitatively agreed with the experimental results by high-speed camera.

(3) The behavior of oil mists with different particle sizes can be analyzed by using the coarse graining ratio as a parameter. This enables investigation of chamber structures in accordance with the particle size of the target oil mist.

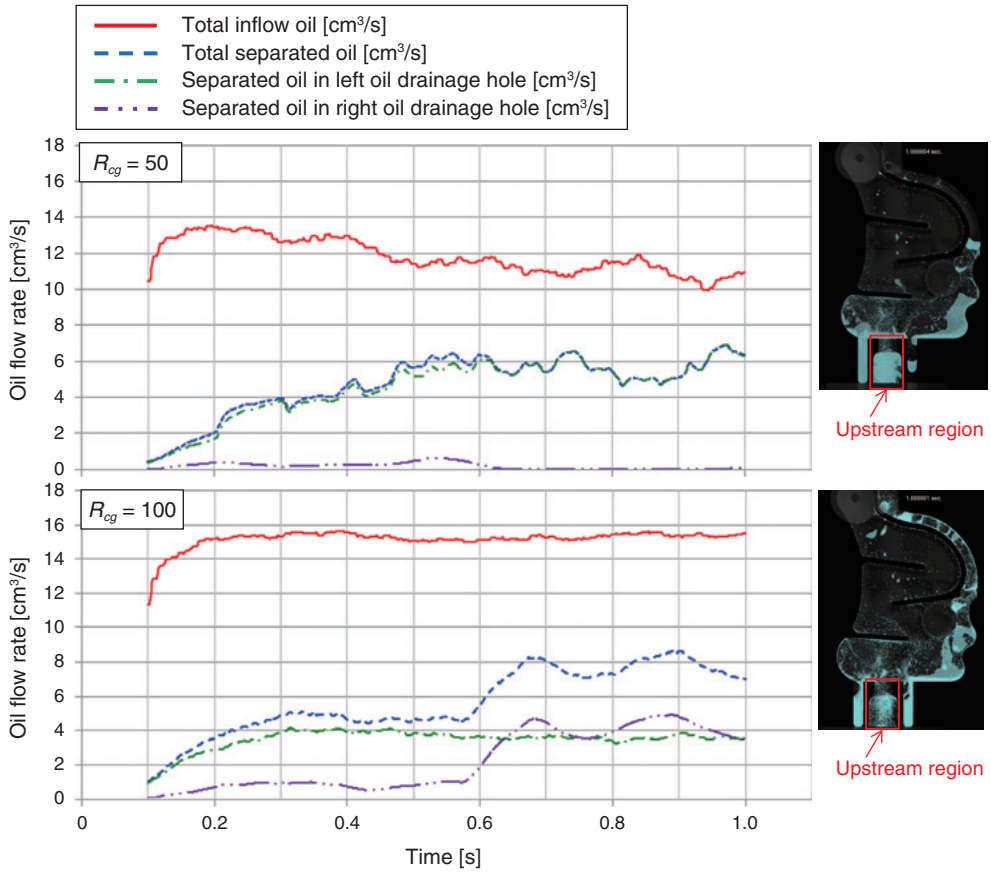

Fig. 14 Comparison of oil flow rate between R_{cg} = 50 and R_{cg} = 100

7. Afterword

Future plans include modeling the wall impact behavior of micro-droplets and the creation of analysis techniques that reflect the particle size distribution of the oil mist in order to quantitatively predict the oil separation capability.

Reference

(1) Satoh, K., Ishikawa, M., Matsuoka, T.: Development of Method of Predicting Efficiency of Oilmist Separator, Transactions of Society of Automotive Engineers of Japan, Vol. 30, No. 2, p. 75-80 (1999) (in Japanese)
(2) Endo, K., Kobayashi, A., Sudo, M.: The Development and Realization of Compact Oil Mist Separator with High Performance, JSAE Annual Congress Proceedings, No. 62-07, p. 13-16 (2007) (in Japanese)
(3) http://www.prometech.co.jp/particleworks.html
(4) Koshizuka, S.: Numetrical Analysis of Flow using Particle Method, Nagare 21, p. 230-239 (2002) (in Japanese)
(5) Koshizuka, S.: Particle Methods (Computational dynamics lecture series), The Japan Society for Computational Engineering and Science, Maruzen Publishing Co., Ltd, 156p. (2005) (in Japanese)
(6) Takagi, M.: The Present Situation and Issue on Fuel Spray Simulation, Papers of National Maritime Research Institute, Vol. 8, No. 2, p. 209-214 (2008) (in Japanese)

■ Author ■

Makoto HAGA

Takumi KASAHARA